JMEPEG (2005) 14:435-440
DOI: 10.1361/105994905X56197

1059-9495/$19.00

Antimicrobial Properties of Diamond-like Carbon-Silver-Platinum Nanocomposite Thin Films

R.J. Narayan, H. Abernathy, L. Riester, C.J. Berry, and R. Brigmon

(Submitted April 27, 2005; in revised form May 12, 2005)

Silver and platinum were incorporated within diamond-like carbon (DLC) thin films using a multicomponent target pulsed laser deposition process. Transmission electron microscopy of the DLC-silver and DLC-platinum composite films reveals that these films self-assemble into particulate nanocomposite structures that possess a high fraction of sp^3-hybridized carbon atoms. Nanoindentation testing of DLC-silver nanocomposite films demonstrates that these films possess hardness and Young's modulus values of approximately 35 and 350 GPa, respectively. DLC-silver-platinum films demonstrated exceptional antimicrobial properties against *Staphylococcus* and *Pseudomonas aeruginosa* bacteria.

Keywords diamond-like carbon, pulsed-laser deposition, thin films

1. Introduction

Biomedical researchers have created advanced materials over the past three decades by selecting bulk materials with appropriate fracture toughness, bulk modulus and durability, and performing surface modification to improve biocompatibility, wear resistance, and corrosion resistance. One ceramic coating with tremendous potential for medical applications is diamond-like carbon (DLC). The term diamond-like carbon (DLC) describes hydrogen-free hard carbon solids that possess a cross-linked, noncrystalline network of sp^2- and sp^3- hybridized carbon atoms (Ref 1). The friction and wear coefficients of DLC are lower than those of diamond, and are among the lowest recorded to date (static coefficient of friction = 0.006). DLC also offers transparency to light ranging from deep ultraviolet to far infrared (IR). In addition, DLC films are amorphous, atomically smooth, and do not contain open corrosion paths to the underlying substrate.

Diamond-like carbon thin films have also been shown to possess excellent cell compatibility. For example, in vitro studies of diamond-like carbon films involving mouse peritoneal macrophages, mouse fibroblasts, human myeloblastic ML-1 cells, osteoblast-like cells, and human embryo kidney 293 cells have demonstrated the absence of an inflammatory response (Ref 2-5). Morphological examination and biochemical data suggest that DLC-exposed cells undergo no cellular damage. For example, osteoblast-like cells exposed to DLC coatings did not demonstrate any change in the creation of alkaline phosphatase, type I collagen, and osteocalcin (Ref 6). In addition, neuronal growth readily occurs on DLC surfaces (Ref 7). Diamond-like carbon thin films have been recently considered for a variety of cardiovascular, orthopaedic, ophthalmic, biosensor, and implantable microelectromechanical system applications, which allow for improved device lifetimes and unique interactions with the biological environment.

Pulsed laser deposition of diamond-like carbon involves laser ablation of a sp^2 bonded carbon target, which results in the formation of a sp^3 bonded film. The most common target material is high purity graphite; other target materials have included pressed diamond powder, glassy carbon, and polymer (Ref 8-10). Pure carbon sources lead to pure DLC films, whereas hydrocarbon sources lead to DLC films with significant hydrogen and/or hydrocarbon incorporation. The reported growth rates of DLC films deposited using a 248 nm excimer laser are on the order of 0.01 nm/pulse (Ref 11). Laser processing of diamond-like carbon thin films involves several interdependent factors, which include: (a) kinetic energy of the carbon species, (b) background pressure, and (c) substrate temperature. These parameters have tremendous bearing on diamond-like carbon film properties, including the sp^3/sp^2 ratio, the adhesion of the DLC film to the substrate, and the amount of sp^2 clustering (Ref 12).

A variant of the conventional pulsed laser deposition process has recently been developed to incorporate biofunctional metals during DLC film deposition. Briefly, a single multicomponent target is loaded into the pulsed laser deposition chamber. This target contains pure graphite that is covered by a piece of the desired modifying element (Fig. 1). The focused laser beam sequentially ablates the graphite target component and the modifying element target component to form composite layers. The metal composition in these films can be controlled through altering the following parameters: (a) the scanning radius of the laser beam on the target surface, (b) the laser beam position, (c) the position of the circular target, (d) the size of the metal piece on the target, and (e) the laser energy density. The fraction of metal atoms incorporated into the dia-

This paper was presented at the International Symposium on Manufacturing, Properties, and Applications of Nanocrystalline Materials sponsored by the ASM International Nanotechnology Task Force and TMS Powder Materials Committee on October 18-20, 2004 in Columbus, OH.

R.J. Narayan and **H. Abernathy,** School of Materials Science and Engineering, Georgia Institute of Technology, Atlanta, GA 30332-0245; **L. Riester,** Metals and Ceramics Division, Oak Ridge National Laboratory, Oak Ridge, TN 37831; and **C.J. Berry** and **R. Brigmon,** Environmental Biotechnology Section, Savannah River National Laboratory, Aiken, SC 29808. Contact e-mail: roger.narayan@mse.gatech.edu.

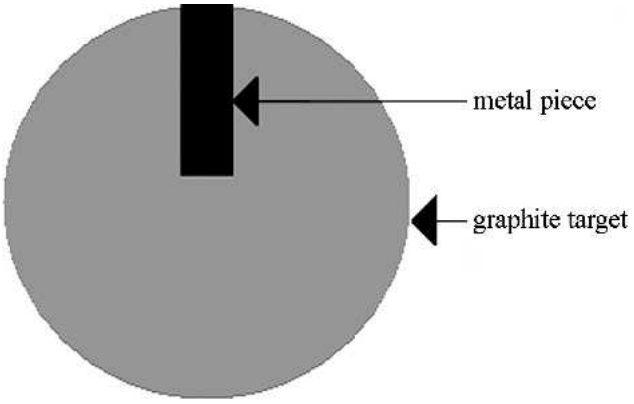

Fig. 1 Schematic illustration of target configuration used in this study

mond-like carbon nanocomposite film can be estimated using the following equation:

$$\frac{\alpha\,\delta\,(l - R_d)}{2\,\pi\,\gamma(1 - R_c)} \qquad \text{(Eq 1)}$$

in which α is the laser ablation ratio, γ is the laser beam scanning radius, R_c is the reflectivity of carbon, R_d is the reflectivity of the metal strip, and δ is width of the metal piece. Several diamond-like carbon-silver nanocomposite films have been prepared using this modified pulsed laser deposition process. These films were examined using transmission electron microscopy, electron energy loss spectroscopy, visible Raman spectroscopy, nanoindentation, and microbial biofilm attachment testing.

2. Experimental

Several 1 × 1 cm pieces of silicon (100) were cleaned in acetone and methanol within an ultrasonic cleaner. The silicon substrates were subsequently dipped in hydrofluoric acid to remove silicon oxide, which resulted in a hydrogen-terminated surface. The Lambda Physik (Göttingen, Germany) LPX 200 KrF (λ = 248 nm) excimer laser was used for ablation of the multicomponent target. Pieces of silver and platinum were placed over the graphite target, which was rotated at 5 rpm throughout the deposition. The laser was operated at a frequency of 10 Hz and a pulse duration of 25 ns. The laser energy output of 215 mJ and laser spot size of 0.043 cm^2 imparted an average energy density of ~5 J/cm^2 to the target. The target-substrate distance was maintained at 4.5 cm.

High-resolution Z-contrast images were obtained using a JEOL (Tokyo, Japan) 2010 F scanning transmission electron microscope (STEM) equipped with field emission gun and Gatan Image Filter (GIF). In STEM-Z contrast imaging, an image is formed by collecting large-angle scattered electrons using an annular detector. The resulting contrast is proportional to atomic number squared (Z^2). Parallel electron energy loss spectroscopy was used to obtain information on carbon bonding; spectra were collected from zero loss up to 1000 eV energy loss. MicroRaman spectra were obtained using an argon ion laser operating at 483-514 nm. The Nanoindenter II system (MTS Instruments, Oak Ridge, TN) was used to assess hardness and Young's modulus of the films.

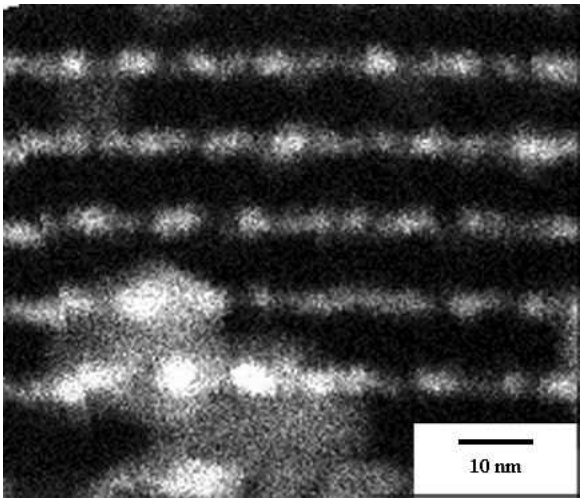

Fig. 2 Dark-field Z-contrast image of diamond-like carbon-silver nanocomposite film

Biofilm attachment studies were done using three microorganisms, *Pseudomonas aeruginosa* (American Type Culture Collection, Manassas, VA), *Staphylococcus sp* (wild type), and *Candida* (wild type) grown in liquid media. Organisms were grown in nutrient broth (Becton Dickinson Co., Franklin Lakes, NJ) at 37 °C for 15 min under 15 pounds pressure on a shaker platform. When log phase growth was obtained, 1 square centimeter DLC-silver, DLC-silver-platinum, and control chips were rinsed with ethyl alcohol, aseptically added to the media, and incubated for 24, 48, and 72 h. Incubated materials were then rinsed three times in formaldehyde-agarose (FA) buffer [10 g Difco #223142 in 1 L deionized ultrafiltered (0.2 um) water, pH = 7.2], vortexed for 1 min, and then rinsed twice more in FA buffer. Samples were then heat fixed at 60 °C for 12 min, stained with 4′-6-diamidino-2-phenylindole dihydrochloride (Becton Dickinson Co., Franklin Lakes, NJ) for 5 min and rinsed with FA buffer. Stained microbial cells were counted, examined, and photographed using a Axioskop2 plus epifluorescent microscope (Carl Zeiss AG, Oberkochen, Germany) and a 510 Meta laser scanning microscope (Carl Zeiss AG, Oberkochen, Germany) using the appropriate filter sets.

3. Results and Discussion

3.1 Transmission Electron Microscopy

Z-contrast STEM provides unique information on nanostructured composite thin films (Ref 13). An image is formed by scanning a 2.2 Å probe across the sample. The Z-contrast signal is collected from a high angle annular detector, and the electron signal scattered through large angles (typically 75-150 mrad) is analyzed. Contrast is proportional to the atomic number (Z) squared. For example, the silver:carbon contrast is over 60:1 and the platinum:carbon contrast is 169:1. Dark field Z-contrast images of diamond-like carbon-silver and diamond-like carbon-platinum nanocomposite films are shown in Fig. 2 and 3, respectively. The bright regions correspond to the higher atomic number metal regions, and the dark regions correspond to the DLC matrix. The noble metals are dispersed as nearly spherical metal clusters in the diamond-like carbon matrix. The average size of these nanocrystalline particles varies

between 3 and 5 nm. These images demonstrate that noble metals are segregated into nanoparticle arrays within the diamond-like carbon matrix.

Electron energy loss spectra between 280-310 eV were acquired. The sp^3 fraction was determined from the K edge loss spectra using an empirical technique developed by Cuomo et al. (Ref 14). In this technique, the peak, in the region from 285-290 eV, results from excitation of electrons from the 1*s* ground state to the vacant π^* antibonding state. The peak, in the region above 290 eV, results from excitation to the higher σ^* state. The ratio of the integrated areas under these two energy windows is approximately proportional to the relative number of π and σ^* orbitals. Using this information, the atomic fraction of sp^2 bonded carbon (x) can be determined using the expression:

$$\frac{[I(\pi)/I(\sigma)]_s}{[I(\pi)/I(\sigma)]_r} = \frac{3x}{(4-x)} \quad \text{(Eq 2)}$$

in which $I(\pi)$ is the intensity in the range from 284 to 289 eV and $I(\sigma)$ is the integrated intensity in the range from 290 to 305 eV. The subscripts s and r refer to the ratio determined for the DLC specimen and a reference material with 100% sp^2 bonding, respectively. The sp^3 content was determined to be 63% for a diamond-like carbon film on silicon (100). The sp^3 content was determined to be 47% for a diamond-like carbon-silver nanocomposite film on Si (100) (Fig. 4). This data suggests that a moderate reduction in sp^3 content occurs in the metal-alloyed films.

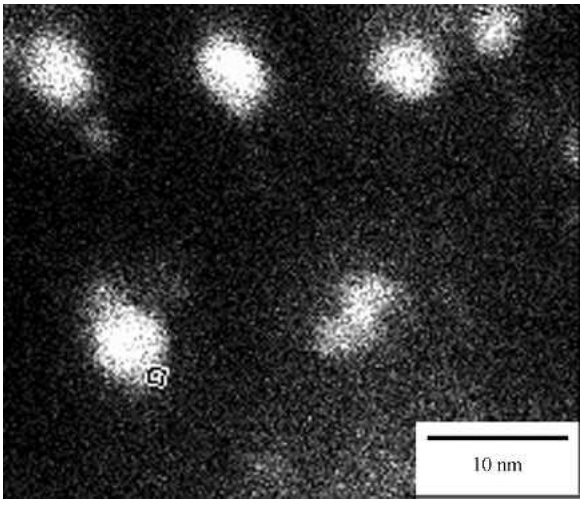

Fig. 3 Bright-field Z-contrast image of diamond-like carbon-platinum nanocomposite film

3.2 Raman Spectroscopy

Adhesion of diamond-like carbon thin films is dependent on several factors, including film stress, film/substrate chemical bonding, and substrate topology (Ref 15-17). Large internal compressive stresses as high as 10 GPa have been observed in diamond-like carbon thin films, regardless of the deposition process used. These stresses limit maximum film DLC thickness to 0.1-0.2 μm, and prevent widespread medical use. Lifshitz et al. have attributed these stresses to "subplantation" (low energy subsurface implantation) of carbon ions during diamond-like carbon film growth (Ref 18, 19). They suggest that carbon ions with energies between 10 and 1000 eV undergo shallow implantation to depths of 1-10 nm during film growth. Carbon species are trapped in subsurface sites due to restricted mobility. This process leads to the development of very large internal compressive stresses.

The Raman spectra of diamond-like carbon thin films contain characteristic peaks that reflect carbon bonding and internal stress. All of the spectra show the following: (a) a broad hump centered in the 1510-1557 cm^{-1} region, known as the G-band, and (b) a small shoulder at 1350 cm^{-1}, known as the D-band. The G-band is the optically allowed E_{2g} zone center mode of crystalline graphite, and is typically observed in diamond-like carbon films. The D-band is the A_{1g} mode of graphite.

High-quality diamond-like carbon films demonstrate the following: (a) a relatively symmetrical G-band, and (b) a lesser D-band, suggesting an absence or a low amount of graphite clusters. The presence of metal atoms leads to a shift in the G-peak to lower wave numbers and a slight increase in the D-peak height (Fig. 5). The G peak position shift can be produced by a decrease in sp^3 content, an increase in graphitic

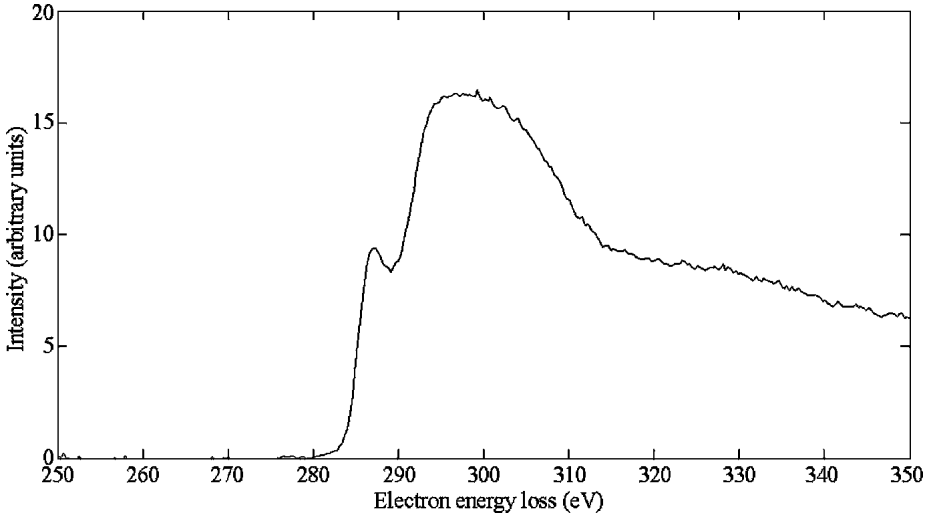

Fig. 4 Electron energy loss near the carbon-K edge of diamond-like carbon-silver nanocomposite film

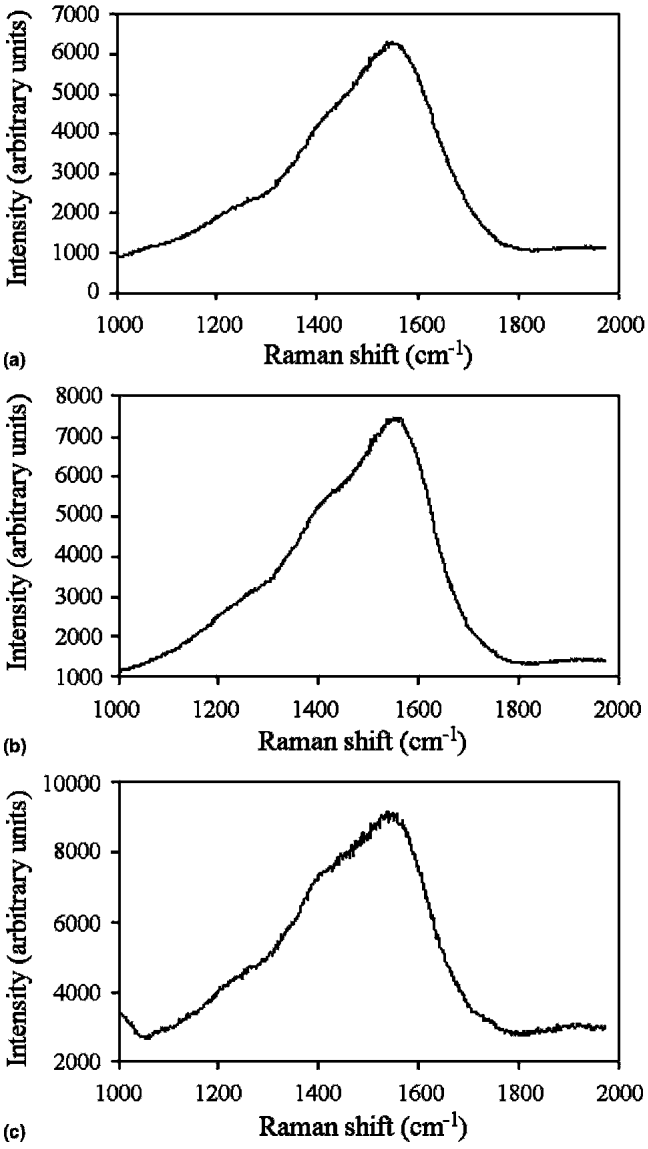

Fig. 5 Visible Raman spectra of (a) diamond-like carbon film, (b) diamond-like carbon-silver nanocomposite film, and (c) diamond-like carbon-platinum nanocomposite film

cluster size within the film, and/or a decrease in compressive stress within the film (Ref 20, 21). Silver and platinum have significantly smaller elastic moduli than diamond-like carbon, and noble metal nanoparticles may be expected to absorb stresses from the diamond-like carbon matrix.

3.3 Nanoindentation

During nanoindentation, the modulus of the coated sample approached that of the uncoated sample at roughly 500 nm (~2/3 of the film thickness). Substrate effects were observed at indentation depths of 100 nm. The nanohardness and Young's modulus values for the diamond-like carbon-silver nanocomposite film were determined to be ~35.4 and ~343.5 GPa, respectively. These values are similar to those observed in layered WC/DLC and TiC/DLC composites prepared using electron cyclotron resonance chemical vapor deposition or magnetron sputtering techniques (~27 GPa) and are significantly greater than those observed in a-C:H-copper coatings prepared using plasma-enhanced chemical vacuum deposition (PECVD) or hybrid microwave plasma-assisted chemical vapor deposition/sputtering techniques (~10 GPa) (Ref 22-26).

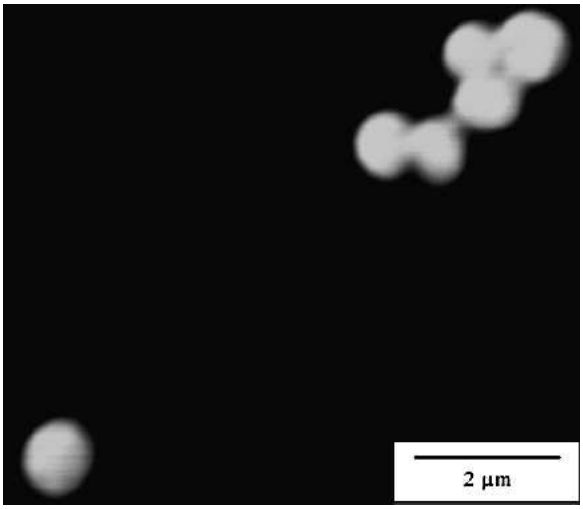

Fig. 6 Laser scanning confocal micrograph of *Staphylococcus sp.* on the surface of a diamond-like carbon-silver film. Free-standing planktonic bacteria and biofilm-forming clusters were observed.

3.4 Biofilm Attachment Studies

The introduction of implantable medical devices into the body have been shown to greatly increase the risk of infection. Infections involving artificial organs, synthetic vessels, joint replacements, or internal fixation devices usually require reoperation. Some infections are more serious than others; infected cardiac, abdominal, and extremity vascular prostheses result in amputation or death (Ref 27, 28).

Bacteria form a glycocalyx, an adherent coating that forms on all foreign materials placed in vivo (Ref 29-31). This 5-50 μm thick glycoprotein-based coating protects bacteria through a diffusion limitation process, and serves to decrease their antibiotic sensitivity by 10-100 times. In addition, the constituents of many alloys and polymers can inhibit both macrophage chemotaxis and phagocytosis. Finally, tissue damage caused by surgery and foreign body implantation further increases the susceptibility to infection.

The sustained delivery of silver ions into the local microenvironment of implants systemic side effects and exceeds usual systemic concentrations by several orders of magnitude (Ref 32-34). Silver nanoparticles have been shown to possess an unsurpassed antimicrobial spectrum, with efficacy against 150 different pathogens. Silver ions bind strongly to electron donor groups on sulfur-, oxygen- or nitrogen-containing enzymes. These ions displace other cations (e.g., Ca^{2+}) important for enzyme function. In addition, nanocrystalline silver also provides broad-spectrum fungicidal action and very low silver ion concentrations are required for microbicidal activity (in the range 10^{-9} mol/l). Films containing both silver and platinum may demonstrate enhanced antimicrobial activity due to formation of a galvanic couple that accelerates silver ion release (Ref 35).

The results of the biofilm attachment study showed a significant difference in the amount of microbial colonization per

unit area between uncoated silicon (100) substrates and DLC-silver and silver-platinum nanocomposite films. Microbial colonization varied with organism type, incubation period, and composite film type. The gram-negative bacteria *Pseudomonas aeruginosa* produced well developed biofilms after 48 h that were difficult to quantify. The gram positive *Staphylococcus sp* also produced a quantifiable biofilm after 24, 48, and 72 h. The eukaryote, *Candida* wild type, produced sporadic biofilms at all incubation periods, which were difficult to quantify. Using rich media and long incubation times, impacted biofilm formation on the composites and untreated materials was observed (Fig. 6). The DLC-silver-platinum nanocomposite film demonstrated a one order of magnitude lower surface microbial density in gram-positive bacteria concentration than the uncoated silicon substrate. Samples showed a difference of between 100% to half an order of magnitude lower colonization rates on the DLC-metal nanocomposite films than on the uncoated silicon substrates.

4. Conclusions

Diamond-like carbon-silver and diamond-like carbon-silver-platinum nanocomposite films were prepared using a novel multicomponent target pulsed laser deposition process. Silver and platinum do not chemically bond with carbon; instead, these metals form nanoparticle arrays within the diamond-like carbon matrix. This self-assembled morphology can be attributed to the high surface energy of noble metals relative to carbon. Ostwald ripening is prevented, and the resulting metal nanoparticles possess uniform size. Raman spectroscopy data suggest these films contain a reduction in internal compressive stress values from those observed in pure diamond-like carbon. Silver and platinum exhibit significantly smaller elastic moduli than diamond-like carbon and may absorb compressive stress from the diamond-like carbon matrix. Nanoindentation testing of the DLC-metal nanocomposite films demonstrates that these films possess hardness and Young's modulus values as high as 35 and 350 GPa, respectively. Finally, diamond-like carbon-silver-platinum nanocomposites exhibit significant antimicrobial efficacy against *Staphylococcus* and *Pseudomonas aeruginosa* bacteria. It is believed that platinum, which is more noble than silver, forms a galvanic couple inside the in vitro biofilm testing environment. Silver release (and, by extension, antimicrobial function) is greatly increased in these diamond-like carbon-silver-platinum nanocomposite films. The in vitro antimicrobial susceptibility of several bacterial and fungal pathogens to diamond-like carbon-biofunctional metal coatings is currently being assessed.

References

1. J. Robertson, Diamond-like Amorphous Carbon, *Mater. Sci. Eng. R,* Vol 37 (No. 4-6), 2002, p 129-281
2. M. Allen, B. Myer, and N. Rushton, In Vitro and In Vivo Investigations into the Biocompatibility of Diamond-Like Carbon (DLC) Coatings for Orthopedic Applications, *J. Biomed. Mater. Res.,* Vol 58 (No. 3), 2001, p 319-328
3. S. Linder, W. Pinkowski, and M. Aepfelbacher, Adhesion, Cytoskeletal Architecture and Activation Status of Primary Human Macrophages on a Diamond-Like Carbon Coated Surface, *Biomaterials,* Vol 23 (No. 3), 2002, p 767-773
4. E. Liu, B. Blanpain, J.P. Celis, J.R. Roos, G. Alvarez Verven, and T. Priem, Tribological Behaviour and Internal Stress of Diamond Coating Deposited with a Stationary DC Plasma Jet, *Surf. Coat. Technol.,* Vol 80 (No. 3), 1996, p 264-270
5. L.A. Thomson, F.C. Law, N. Rushton, and J. Franks, Biocompatibility of Diamond-Like Carbon Coating, *Biomaterials,* Vol 12 (No. 1), 1991, p 37-40
6. M. Allen, B. Myer, and N. Rushton, In Vitro and In Vivo Investigations into the Biocompatibility of Diamond-Like Carbon (DLC) Coatings for Orthopedic Applications, *J. Biomed. Mater. Res.,* Vol 58 (No. 3), 2001, p 319-328
7. M.J. Ignatius, N. Sawhney, A. Gupta, B.M. Thibadeau, O.R. Monteiro, and I.G. Brown, Bioactive Surface Coatings for Nanoscale Instruments: Effects on CNS Neurons, *J. Biomed. Mater. Res.,* Vol 40 (No. 2), 1998, p 264-274
8. M.B. Guseva, V.G. Babaev, V.V. Khvostov, Z.K. Valioullova, A.Y. Bregadze, A.N. Obraztsov, and A.E. Alexenko, Deposition of Thin Highly Dispersive Diamond Films by Laser-Ablation, *Diam. Relat. Mater.,* Vol 3 (No. 4-6), 1994, p 328-331
9. N. Kikuchi, Y. Ohsawa, and I. Suzuki, Diamond Synthesis by CO_2-Laser Irradiation, *Diam. Relat. Mater.,* Vol 2 (No. 2-4), 1993, p 190-196
10. A.A. Voevodin, S.J.P. Laube, S.D. Walck, J.S. Solomon, M.S. Donley, and J.S. Zabinski, Pulsed-Laser Deposition of Diamond-Like Amorphous-Carbon Films from Graphite and Polycarbonate Targets, *J. Appl. Phys.,* Vol 78 (No. 6), 1995, p 4123-4130
11. A.A. Voevodin and M.S. Donley, Preparation of Amorphous Diamond-Like Carbon by Pulsed Laser Deposition: A Critical Review, *Surf. Coat. Technol.,* Vol 82 (No. 3), 1996, p 199-213
12. A.A. Voevodin, M.S. Donley, J.S. Zabinski, and J.E. Bultman, Mechanical and Tribological Properties of Diamond-Like Carbon Coatings Prepared by Pulsed Laser Deposition, *Surf. Coat. Technol.,* Vol 77 (No. 1-3), 1995, p 534-539
13. S. Lopatin, S.J. Pennycook, J. Narayan, and G. Duscher, Z-Contrast Imaging of Dislocation Cores at the GaAs/Si Interface, *Appl. Phys Lett.,* Vol 81 (No. 15), 2002, p 2728-2730
14. J. Bruley, D.B. Williams, J.J. Cuomo, and D.P. Pappas, Quantitative Near-Edge Structure-Analysis of Diamond-Like Carbon in the Electron-Microscope Using a 2-Window Method, *J. Microscopy (Oxford),* Vol 180 (No. 1), 1995, p 22-32
15. E.H. A. Dekempeneer, R. Jacobs, J. Smeets, J. Meneve, L. Eersels, B. Blanpain, J. Roos, and D.J. Oostra, RF Plasma-Assisted Chemical Vapor-Deposition of Diamond-Like Carbon- Physical and Mechanical-Properties, *Thin Solid Films,* Vol 217 (No. 1-2), 1992, p 56-61
16. K. Bewilogua, D. Dietrich, G. Holzhuter, and C. Weissmantel, Structure of Amorphous-Carbon Films, *Phys. Status Solidi A,* Vol 71 (No. 1), 1982, p 57-59
17. D.G. McCulloch, D.R. McKenzie, and C.M. Goringe, Ab Initio Simulations of the Structure of Amorphous Carbon, *Phys. Rev. B,* Vol 61 (No. 3), 2000, p 2349-2355
18. Y. Lifshitz, Hydrogen-Free Amorphous Carbon Films: Correlation Between Growth Conditions and Properties, *Diam. Relat. Mater.,* Vol 5 (No. 3-5), 1996, p 388-400
19. Y. Lifshitz, G.D. Lempert, E. Grossman, I. Avigal, C. Uzansaguy, R. Kalish, J. Kulik, D. Marton, and J.W. Rabalais, Growth Mechanisms of DLC Films from C+ Ions- Experimental Studies, *Diam. Relat. Mater.,* Vol 4 (No. 4), 1995, p 318-323
20. B.K. Tay and P. Zhang, On the Properties of Nanocomposite Amorphous Carbon Films Prepared by Off-Plane Double Bend Filtered Cathodic Vacuum Arc, *Thin Solid Films,* Vol 420, 2002, p 177-184
21. V.V. Uglova, V.M. Anishchik, Y. Pauleau, A.K. Kuleshov, F. Thièry, J. Pelletier, S.N. Dub, and D.P. Rusalsky, Relations Between Deposition Conditions, Microstructure and Mechanical Properties of Amorphous Carbon-Metal Films, *Vacuum,* Vol 70 (No. 2-3), 2003, p 181-185
22. Y. Pauleau and F. Thièry, Deposition and Characterization of Nanostructured Metal/Carbon Composite Films, *Surf. Coat. Technol.,* Vol 180-181, 2004, p 313-322
23. D. Sheeja, B.K. Tay, J.Y. Sze, L.J. Yu, and S.P. Lau, A Comparative Study Between Pure and Films Prepared by FCVA Technique Biasing Al-Containing Amorphous Carbon with High Substrate Pulse, *Diamond Relat. Mater.,* Vol 12 (No. 10-11), 2003, p 2032-2036
24. H. Rusli, S. F. Yoon, Q. F. Huang, J. Ahn, Q. Zhang, H. Yang, Y. S. Wu, E. J. Teo, T. Osipowicz, and F. Watt, Metal-Containing Amorphous Carbon Film Development Using Electron Cyclotron Resonance CVD, *Diamond Relat. Mater.,* Vol 10 (No. 2), 2001, p 132-138
25. Rusli, S.F. Yoon, H. Yang, J. Ahn, Q.F. Huang, Q. Zhang, Y.P. Guo,

C.Y. Yang, E.J. Yeo, A.T.S. Wee, A.C. H. Huan, and F. Watt, Tungsten-Carbon Thin Films Deposited Using Screen Grid Technique in an Electron Cyclotron Resonance Chemical Vapour Deposition System, *Surf. Coat. Technol.,* Vol 123 (No. 2-3), 1999, p 134-139
26. C. Strondl, N.M. Carvalho, J.T.M. De Hosson, and G.J. van der Kolk, Investigation on the Formation of Tungsten Carbide in Tungsten-Containing Diamond-Like Carbon Coatings, *Surf. Coat. Technol.,* Vol 162 (No. 2-3), 2003, p 288-293
27. G. Printzen, Relevance, Pathogenicity and Virulence of Microorganisms in Implant Related Infections, *Injury-Inter. J. Care Injured,* Vol 27 (No. 3), 1996, p 9-15
28. Z.U. Isiklar, G.C. Landon, and H.S. Tullos, Amputation after Failed Total Knee Arthroplasty, *Clin. Orthop. Relat. Res.,* Vol 299, 1994, p 173-178
29. K. Merritt, A. Gaind, and J.M. Anderson, Detection of Bacterial Adherence on Biomedical Polymers, *J. Biomed. Mater. Res.,* Vol 39 (No. 3), 1998, p 415-422
30. C.C. Chang and K. Merritt, Microbial Adherence on Poly(Methyl Methacrylate) Surfaces, *J. Biomed. Mater. Res.,* Vol 26 (No. 2), 1992, p 197-207
31. K.K. Jefferson, What Drives Bacteria to Produce a Biofilm?, *FEMS Microbiol. Lett.,* Vol 236 (No. 2), 2004, p 163-173.
32. R.O. Darouiche, Anti-Infective Efficacy of Silver-Coated Medical Prostheses, *Clin. Infect. Dis.,* Vol 29 (No. 6), 1999, p 1371-1377
33. D.J. Stickler, Biomaterials to Prevent Nosocomial Infections: Is Silver the Gold Standard?, *Curr. Opin. Infect. Dis.,* Vol 13 (No. 4), 2000, p 389-393
34. K.S. Oh, S.H. Park, and Y.K. Jeong, Antimicrobial Effects of Ag Doped Hydroxyapatite Synthesized from Co-Precipitation Route, *Key Eng. Mater.,* Vol 264-268 (No. 1-3), 2004, p 2111-2114
35. D.P. Dowling, A.J. Betts, C. Pope, M.L. McConnell, R. Eloy, and M.N. Arnaud, Anti-Bacterial Silver Coatings Exhibiting Enhanced Activity Through the Addition of Platinum, *Surf. Coat. Technol.,* Vol 163, 2003, p 637-640